BIRL, Industrial Research Laboratory
and The Department of Chemistry
Northwestern University
Evanston, IL 60201

New Fabrication Strategies for Polymer Electrolyte Batteries

Final Report
to Office of Naval Research
Grant No: N00014-94-1-0720
R&T Project: 9332003arp01
(May, 1994 - August, 1996)

ONR Scientific Officer
Dr. Robert Nowak
Office of Naval Research
Ballstone Tower One
800 North Quincy Street
Arlington, Virginia 22217-5660

Principal Investigators:
D. F. Shriver and S. Vaynman

May 1, 1997

TABLE OF CONTENTS

INTRODUCTION/OBJECTIVE 1
RESULTS AND DISCUSSION 2
1. Synthesis and Characterization of Electrolytes 2
1.1. $(a\text{-}PEO)_{38}Li[Al(OSiEt_3)_4]$ 2
1.2. $(MEEP)_4LiCF_3SO_3$ 3
1.3. Aluminosilicate Polyelectrolyte 3
2. Film Fabrication by Ultrasonic spray 4
2.1. Effect of Ultrasound on Molecular Weight of Polymer 5
2.2. Morphology of Deposited Films 8
3. Cell Fabrication 14
4. Cell Testing 15
4.1. $Li/(a\text{-}PEO)_{38}Li[Al(OSiEt_3)_4]/ LixMn_2O_4$ Cells 15
4.2. $Li/(MEEP)_4LiCF_3SO_3/Li_xMnO_2$ Cells 20
4.3. Aluminum Polyelectrolyte Cells 24
SUMMARY 25
REFERENCES 25

INTRODUCTION/OBJECTIVE

Rechargeable lithium batteries are widely recognized as excellent candidates as power sources for applications where energy and power density are critical.[1] One promising lithium battery technology is based on polymer electrolytes.[1-3] The often cited advantages of polymer electrolyte batteries include: stability toward electrodes that provide high energy density, greater safety than liquid electrolyte batteries, ruggedness, low self-discharge rates, ability to accommodate temperature excursions, and moderate cost. Despite these predictions, polymer electrolyte batteries are not yet commercially available. The lack of fully commercial lithium-polymer batteries (other than highly specialized batteries such as those in heart pacemakers) is associated with several factors. One problem is the comparatively low electrolyte conductivity, which can only be partly compensated by use of thin electrolyte films. Another problem is the poor low-temperature conductivity of most polymer electrolytes. A third issue with polymer electrolytes is the relatively low transference number for cations. Our research group has addressed these issues in the development of phosphazene, siloxy and aluminosilicate polyelectrolytes with improved low temperature performance and unity transference number for cations. The complex dielectric and electrochemical properties of these materials have been extensively investigated in our laboratory.[4-9]

The current approaches to the fabrication of solid state lithium cells are based on mechanically joining discrete layers of electrodes and electrolytes. The individual layers are typically produced by a variety of processing techniques. Lithium foil is produced by rolling, and polymer electrolytes and anode films are often formed by doctor blade methods. The films are then laminated together and sealed in an air-tight case. Lithium is sensitive to oxygen, nitrogen and moisture, so considerable care is necessary to exclude these contaminants in the fabrication process.

The objective of this research was to fabricate lithium-polymer batteries by techniques that may produce a thin electrolyte and cathode films and with minimal contamination during fabrication. One such technique, ultrasonic spray was used. Another objective of this research was to test lithium cells that incorporate the new polymer electrolytes and polyelectrolytes developed at Northwestern University.

RESULTS AND DISCUSSION

1. Synthesis and Characterization Of Electrolytes

The polymer electrolytes, synthesized and tested in lithium cells, are listed in Table 1.

Table 1. Electrolytes Tested in Cells

MATERIAL	DESCRIPTION
$(a\text{-}PEO)_{38}Li[Al(OSiEt_3)_4]$	Polymer-salt complex
$(MEEP)_4LiCF_3SO_3$	Polymer-salt complex
Polyether-aluminosilicate	Polyelectrolyte

Electrolytes used in this project were synthesized and prepared as follows.

1.1. $(a\text{-}PEO)_{38}Li[Al(OSiEt_3)_4]$

An electrolyte based on amorphous polyethylene oxide, $(a\text{-}PEO)_{38}Li[Al(OSiEt_3)_4]$, was prepared as follows. The polymer was purified by dialysis to remove oligomeric species and KOH. The purified a-PEO was characterized by FTIR spectroscopy, ^1H NMR, thermogravimetric analysis (TGA) and X-ray diffraction. The molecular weight of the polymer was assessed by Gel Permeation Chromatography (GPC) and viscosimetry. The latter technique indicates a molecular weight of about 53,000, with a polydispersity of 1.39.

TGA under nitrogen gas demonstrated that a-PEO is stable up to about 233°C. Under compressed air, it is stable up to 179 °C. A small amount of the polymer was smeared onto a glass slide and the sample was scanned from 2 to 60° at a scan rate of 1.27°/min using XRD. A broad peak was observed at $2\theta = 21°$, consistent with the amorphous nature of the polymer. Small but sharp peaks were observed at $2\theta = 3.4°$ and 4.4° indicating the presence of some crystalline domains in the polymer sample.

The as-prepared a-PEO has -OH end-groups that are potentially susceptible to reaction with the lithium anode in lithium batteries. Therefore, the -OH groups in a-PEO were converted to $-OCH_3$. Dialysis was carried out for about a week to remove salt impurities from the polymer.

$Li[Al(OSiEt_3)_4]$ was synthesized by reacting excess Et_3SiOH with $LiAlH_4$ (1 M solution in THF). In a typical reaction the two reagents were allowed to stir at room temperature for 1/2 hour and then refluxed for 2 hours. The reaction mixture was then cooled to room temperature. Excess THF and Et_3SiOH were removed in vacuum. The formulation of the waxy salt product was confirmed by FTIR spectroscopy, and NMR (^1H, ^{29}Si, ^{27}Al).

1.2. $(MEEP)_4LiCF_3SO_3$

MEEP, ($[PN(OCH_2CH_2OCH_2CH_2OCH_3)_2]_n$), was prepared by the ring opening polymerization of purified trimer $(PNCl_2)_3$ at 250°C, followed by nucleophilic substitution with $CH_3OCH_2CH_2OCH_2CH_2ONa$ in THF. The polymer was purified by dialysis to remove the NaCl by-product, and characterized by ^{31}P NMR, FTIR spectroscopy, X-ray diffraction, Energy Dispersive Spectroscopy (EDS), viscosimetry and TGA. ^{31}P NMR and FTIR spectroscopy confirmed the identity of the polymer. EDS showed the presence of phosphorus and the absence of chlorine which confirmed the complete removal of NaCl during the purification by dialysis. Using commercially available PEO as standards, the molecular weight of MEEP was determined by GPC to be about 28,000. X-ray diffraction of the MEEP showed a broad peak at $2\theta = 21.5°$ consistent with the amorphous character of the polymer. A smaller and sharper peak was observed at $2\theta = 6°$, suggesting the presence of a semicrystalline oligomeric species. MEEP was found to be thermally stable under both air and nitrogen up to about 215°C indicating substantial resistance to oxidation.

Dissolution of $LiCF_3SO_3$ into MEEP was carried out with THF as the common solvent. The polymer and the salt in the weight ratio of 4 polymer repeat units to 1 formula unit of salt were thoroughly dried and then dissolved in dry THF under a dry nitrogen atmosphere. A clear solution formed in about 1 day. Heating was sometimes necessary to assist the dissolution. In order to prepare a solution with a viscosity appropriate for casting films, the concentration was adjusted by evaporation or addition of THF.

1.3. Aluminosilicate Polyelectrolyte

A polyelectrolyte was prepared by the procedure described in detail in Ref. 9.

Poly(ethylene glycol) ($MW_{av} \approx 200$-900) was reacted with excess sodium hydride, followed by allyl chloride, yielding a,w-bis(allyloxy)poly(ethylene glycol) (1). Hydrosilylation of compound 1 with dimethylchlorosilane in the presence of Karstedt's catalyst (platinum(0) divinyltetramethyl disiloxane) formed a,w-bis(chlorodimethylsilyl) poly(ethylene glycol) (2), which was quantitatively hydrolyzed, producing a,w-bis(hydroxydimethylsilyl)poly(ethylene glycol) (3). Linear polyelectrolytes were then synthesized by the reaction of sodium bis(2-methoxyethoxy)aluminum hydride with a 5% excess of compound 3, to yield $[NaAl(OEOMe)_2(OSiMe_2(CH_2)_3(OE)_xO(CH_2)_3SiMe_2O)_{2/2}]_n$ [Me = CH_3, OE = OCH_2CH_2] (4).

A network polyelectrolyte $[NaAl(OSiMe_3)(OSiMe_2(CH_2)_3(OE)_xO(CH_2)_3 SiMe_2O)_{3/2}]_n$ (5) was prepared by addition of compound 3 (5% excess) to a stirred solution of triethylaluminum and sodium trimethylsilanolate. The complex of cryptand [2.2.2] (4,7,13,16,21,24-hexaoxa-1,10-diazabicyclo [8.8.8]hexacosane), with linear polyelectrolyte 4 was prepared by adding a stoichiometric quantity (1:1 cryptand:Na^+) of cryptand [2.2.2] to 4 or 5 immediately after polymerization, followed by solvent removal

under high vacuum (compound 6). The reactions were carried out under dry nitrogen using standard Schlenk and glovebox techniques, and the products were stored under nitrogen.

The identity of intermediates 1-3 were confirmed by mass spectrometry and $^{13}C/^{1}H$ NMR. The formation of a covalent bond between the aluminum centers and siloxy oxygens was demonstrated by progressive upfield shifts of the ^{29}Si resonance, from d = 31ppm (2) to 15.5 (3) and to d ≈ 0 in the final polymer products 4 and 5. Additionally, ^{27}Al NMR spectra of compounds 4 and 5 exhibited broad signals centered around d » 60-64 ppm, a value indicative of asymmetric, 4-coordinate oxo-aluminum. Polymers 4 and 5 exhibit little if any flow at room temperature. Exposure to atmospheric moisture results in slow hydrolysis of the surface of the linear polymer after 1-2 months; the network polymer remains stable for more than 3 months. AC impedance spectra were collected using polymer pellets approximately 0.1 cm thick and 1.2 cm in diameter sandwiched between stainless steel or tantalum blocking electrodes. Spectra were obtained for the frequency range 5 Hz - 13 MHz over a range of temperatures. The network polyelectrolyte 4 was tested in electrochemical cells.

2. Film Fabrication by Ultrasonic Spray

Ultrasonic Atomizing Nozzle System from Sono-Tek Corporation was used in this project to produce thin films of polymer electrolytes and composite cathodes. This system provides uniform, ultra-fine, low velocity spray over a wide surface. It is capable of delivering a wide variety of materials, such as solutions and particulate suspensions. Atomization of the liquid occurs in the nozzle (Figure 1) as liquid comes in contact with the vibrating nozzle atomizing surface. Drops are formed when the ultrasonic energy exceeds the liquid's surface tension. Drop size distribution is determined by nozzle frequency, liquid surface tension, and liquid density, with frequency being the key factor. The higher the frequency the smaller the drop size. Typically, the drop size distribution from ultrasonic nozzles follows a log-normal distribution curve. Figure 2 shows the drop size distribution for several nozzle frequencies. Since the objective of this project was to make the thinnest film possible, the 120 Hz ultrasonic nozzle, that is supposed to produce the smallest drops, was used in this project.

The success in atomizing a particular liquid ultrasonically is dependent on the nature of the liquid. Pure liquids in general atomize easily. The process is mainly viscosity dependent, although surface tension and volatility also can affect atomization. Organic polymer solutions, that contain long chain polymers, generally do not follow viscosity rules for atomizing. These solutions can be highly cohesive, making them difficult to atomize, irrespective of the amount of input power supplied to the nozzle. In addition, ultrasound may affect the polymer molecular weight. Suspensions and slurries provide the greatest variability with regard to atomizability. This is because these are multicomponent systems. The key factors influencing the atomizability of these materials are size of the particles, the stability of the suspension and the properties of the liquid phase. As a general rule, solids should be at least an order of magnitude smaller in diameter than the

mean diameter of drops produced by nozzle. If stability of the suspension is poor, production of homogeneous film is unlikely. Testing is required to determine when the polymer solution or suspension, such as cathode mixture, can be atomized without chemical degradation. These concerns in respect to fabrication of lithium battery components by ultrasonic spray technique are addressed in the following section.

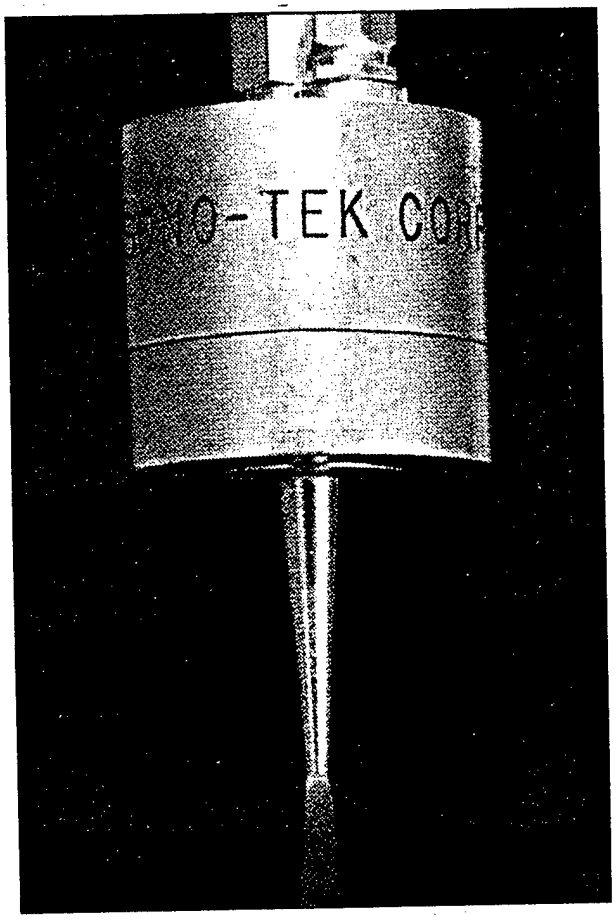

Figure 1. Sono-Tek ultrasonic nozzle.

2.1. Effect of Ultrasound on Molecular Weight of Polymer

Although ultrasonic spray techniques are used with success to spray polymeric materials, it is well known that ultrasonic irradiation can break down polymers. In the initial experiments the influence of ultrasonic spray on the polymeric materials was investigated. In these tests the 2% a-PEO solution in THF was sprayed and molecular weight distributions was determined both before and after spray by gel permeation chromatography to determine the relative fragility of the polymer material. As the test demonstrated, there was very little change in the molecular weight and molecular weight

distribution due to ultrasound treatment. The mean molecular weight of a-PEO before ultrasound spray was 81,446 and after spray was 77,643 (Figures 3, 4). Thus, this test demonstrated that the polymer is sufficiently robust under the spraying conditions we employed.

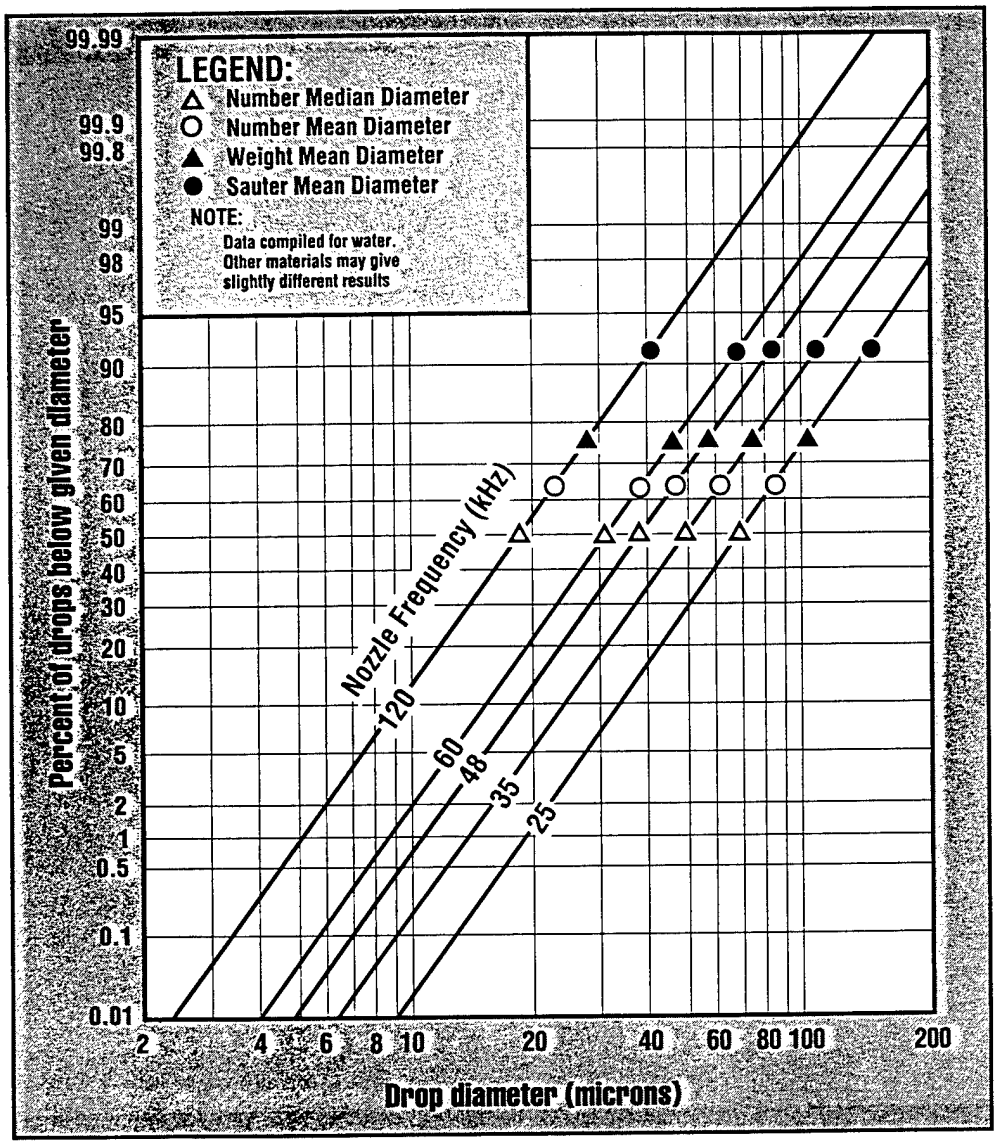

Figure 2. Relationship between water drop size distribution, drop diameter and nozzle frequency for Sono-Tek ultrasonic nozzle.

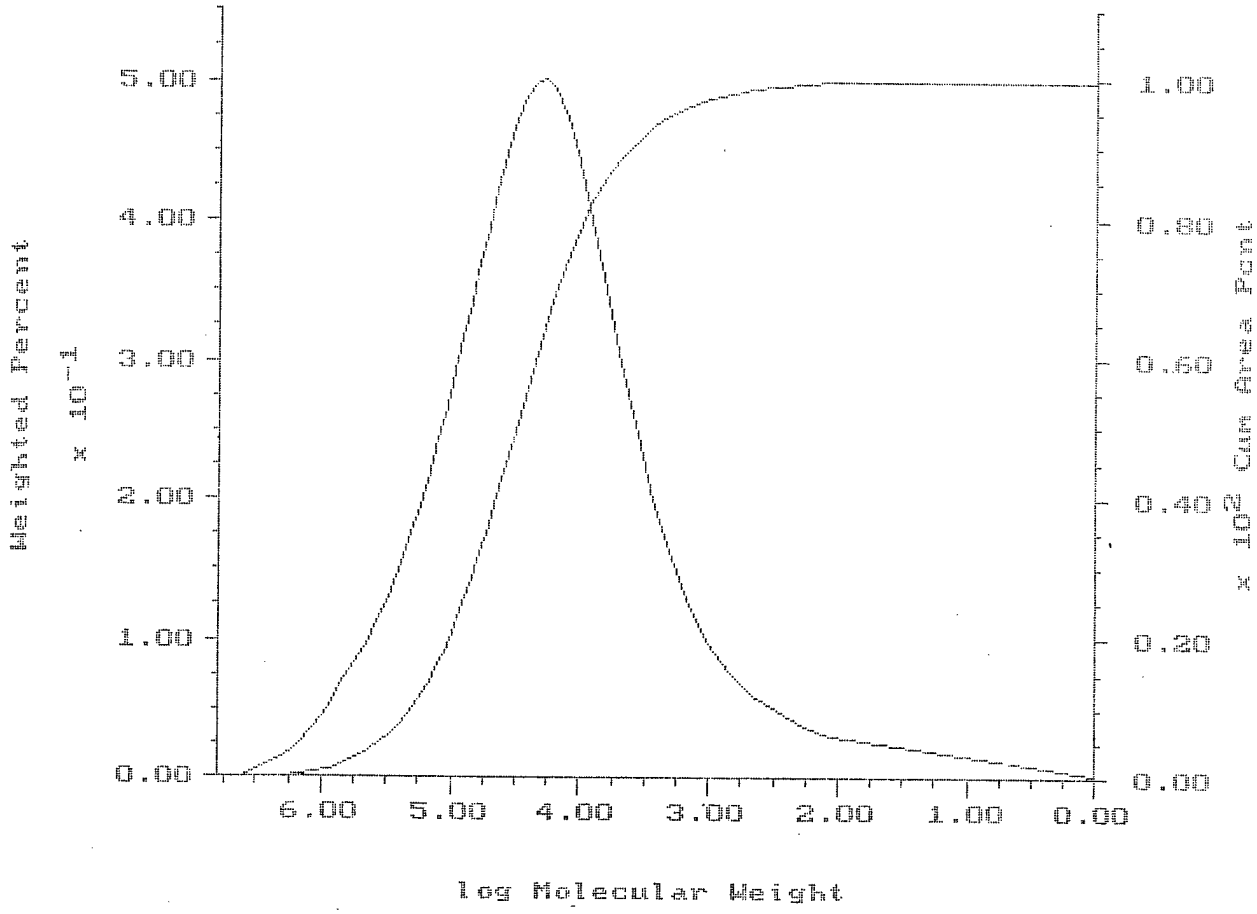

Figure 3. Results of gel permeation chromotography for a-PEO before ultrasonic spray.

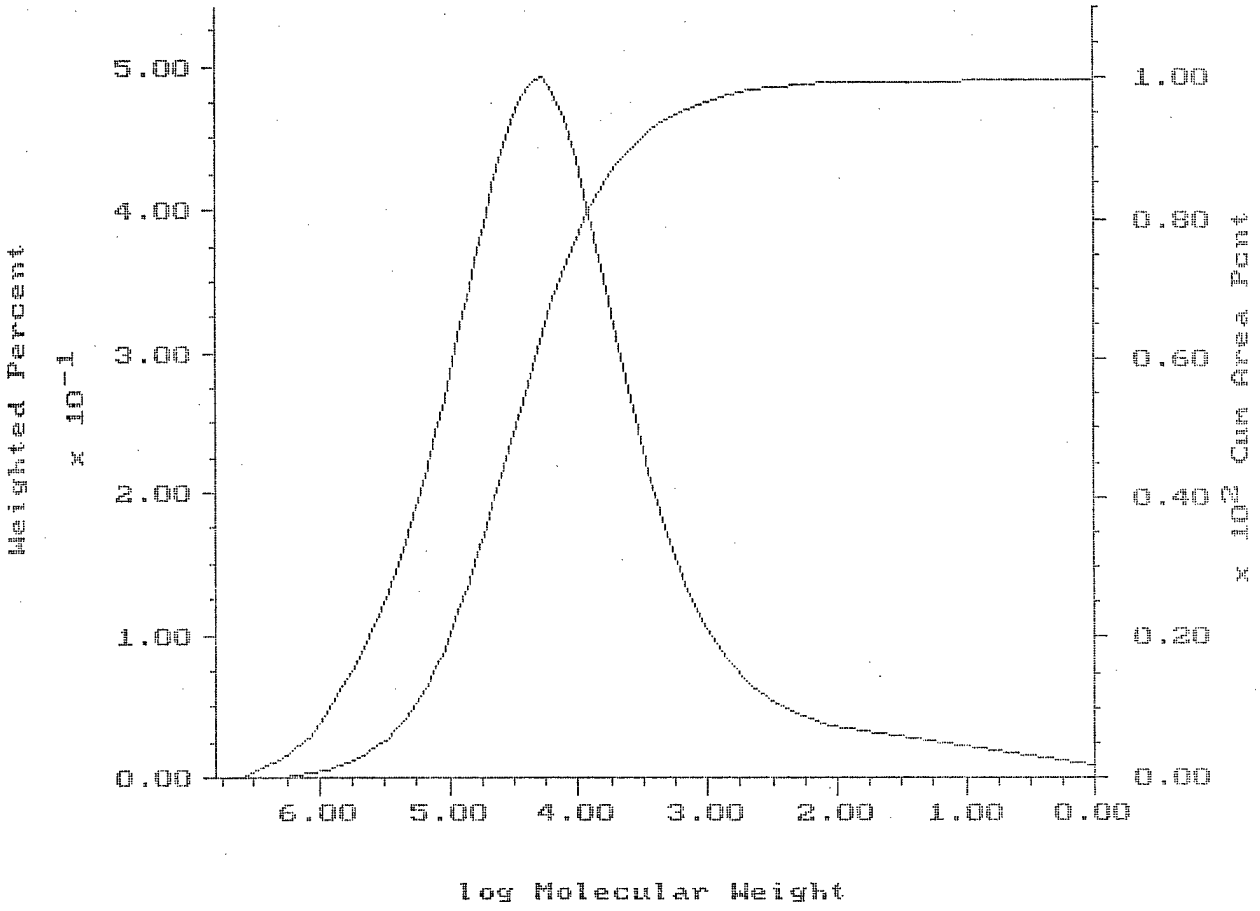

Figure 4. Results of gel permeation chromotography for a-PEO after ultrasonic spray.

2.3. Morphology of Deposited Films

Optical and scanning electron microscopy of ultrasonically deposited polymer and cathode films was performed to determine their morphology. Polymer-solvent and cathode material-solvent ratios were found to be the most important variable during film deposition. Concentration of polymer or cathode material in THF varied from 1 to 5%. The best a-PEO electrolyte film, i.e. uniform and without pinholes, was produced from 2% solution. Figure 5 shows the surface of the film formed from 1% solution. The film is very smooth, however, it has a number of cracks, that are undesirable for battery

applications. Figure 6, shows that a-PEO film formed from 2% solution is not as smooth as film formed from 1% solution, however, it does not have cracks or pinholes. Film formed from 4% solution (Figure 7) consists of flattened remnants of polymer spheres connected to each other. This film has numerous pores. This morphology indicates that drops lost some of the solvent during travel from the nozzle to the surface and became almost dry before they reached the surface. Figure 8 shows the morphology of the polymer electrolyte produced from 5% a-PEO solution in THF. Spheres of polymer are connected to each other. It is obvious that the dry spheres were formed due to the evaporation of solvent before sphere reached the surface. These morphologies are not acceptable for electrolyte film because of the high density of pores. It is probable that increased solvent vapor pressure in the chamber would improve film quality.

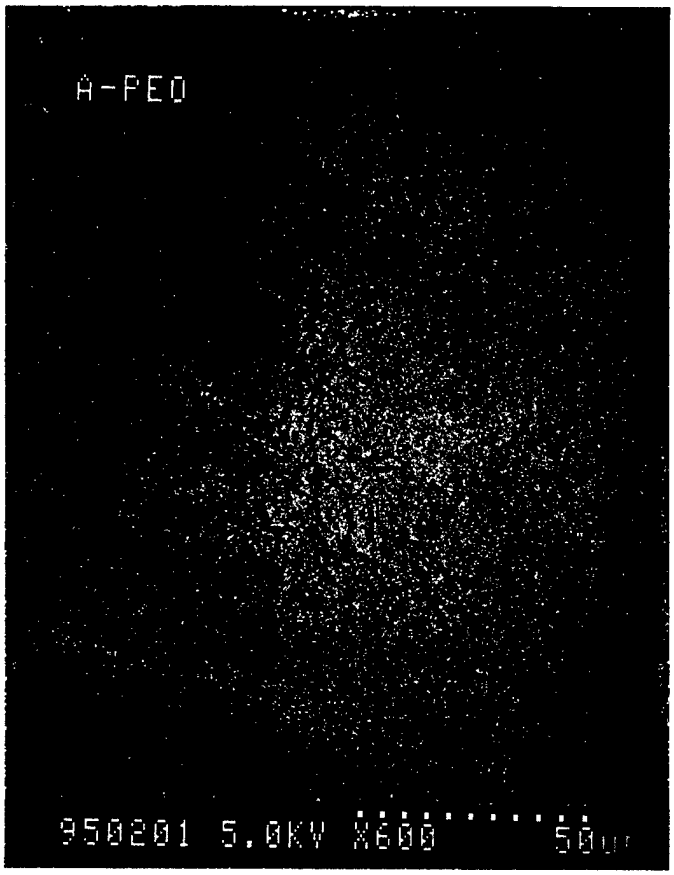

Figure 5. SEM of the film formed by ultrasonic spraying of 1% solution of a-PEO in THF

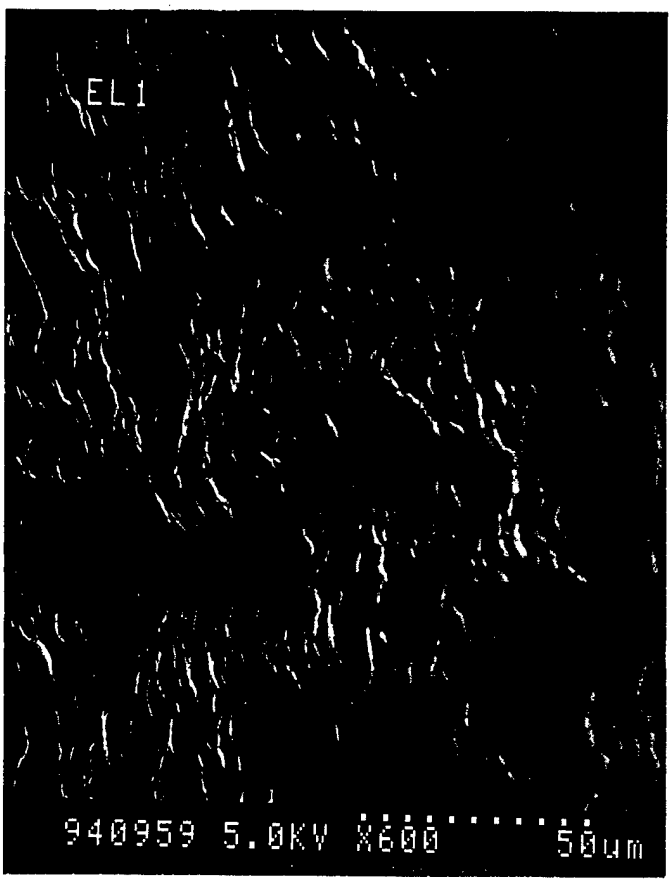

Figure 6. SEM of the film formed by ultrasonic spraying of 2% solution of a-PEO in THF.

Figure 7. SEM of the film formed by ultrasonic spraying of 4% solution of a-PEO in THF.

Figure 8. SEM of the film formed by ultrasonic spraying of 5% solution of a-PEO in THF.

The morphology of the cathode, that contained 80% of Li_xMnO_2 (3 V), 5% of carbon and 15% a-PEO, and which was sprayed as 2% solution in THF (Figure 9), is similar to that of a-PEO in Figure 6. The cathode film that contained less polymer (87% of Li_xMnO_2 (3 V), 5% of carbon and 8% a-PEO) and which was also sprayed from 2% solution (Figure 9) had disconnected particles and numerous pores. This morphology is not optimal for cathode in polymer electrolyte cell. In view of these findings, 2% solutions of polymer and cathode mixtures in THF were used for ultrasonic spray of films used in the project.

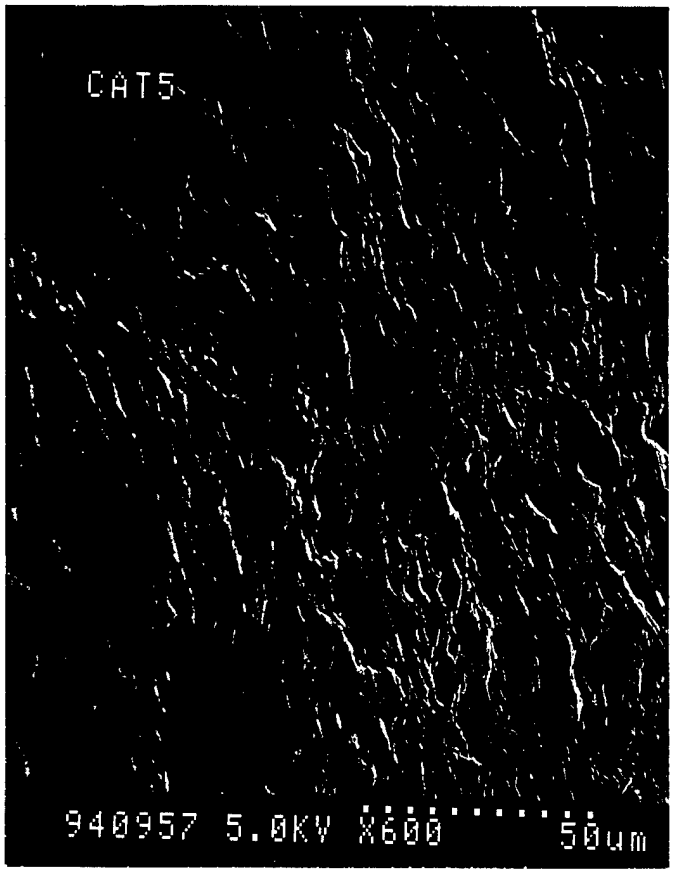

Figure 9. SEM of the cathode film formed by ultrasonic spraying of 5% solution of cathode mixture (80% of Li_xMnO_2 (3 V), 5% of carbon, 15% a-PEO) in THF.

Figure 10. SEM of the cathode film formed by ultrasonic spraying of 5% solution of cathode mixture (87% of Li_xMnO_2 (3 V), 5% of carbon, 8% a-PEO) in THF.

3. Cell Fabrication

Metallic lithium was used as the anode material in all cells.

Composite cathodes were prepared by mixing 80 wt.% oxide (either $Li_xMn_2O_4$ (4 V) or Li_xMnO_2 (3 V), 5 wt.% carbon, and 15 wt.% respective electrolyte. In cells prepared by conventional technique cathode mixture was pressed on a stainless steel disk, or embedded into a metal wire cloth, and then assembled into test cells. The cathode mixture was first dissolved/dispersed in THF in a 2:98 ratio and then ultrasonically sprayed onto the substrate.

Films of polymer-salt-complex (a-PEO-aluminosilicate salt or MEEP-lithium triflate) electrolytes were prepared from THF solutions either by casting directly over

lithium or stainless steel followed by solvent removal under vacuum for 10-14 hours, either by spraying lithium anode with 2% polymer in THF. Thicknesses of the cast film were 70-80 mm. The sprayed film were 40-50 mm. thick. Thinner films produced by either technique had pinholes or other discontinuities.

Aluminosilicate polyelectrolyte is a cross-linked polymer, therefore, an electrolyte film could not be produced by casting from solution or by ultrasonic spray. These polyelectrolyte films were prepared by pressing a small quantity of the material between two stainless steel plates at 80°C for 24 hours. The uniform film was typically 100-125 mm thick. Electrical conductivity measurements were performed on this film and on other films up to 1 mm thick. Further work is needed to devise a convenient method to produce thinner films of this material.

Symmetrical metal/polymer/metal cells were assembled and used to determine the bulk conductivity of the electrolytes (both electrodes made of stainless steel). Investigation of the interfacial interaction between lithium and the polymer electrolyte was carried out on symmetric Li/electrolyte/Li cells.

4. Cell Testing

4.1. $Li/(a\text{-}PEO)_{38}Li[Al(OSiEt_3)_4]/ Li_xMn_2O_4$ Cells

Charge-discharge data for $Li/(a\text{-}PEO)_{38}Li[Al(OSiEt_3)_4] / Li_xMn_2O_4$ cells at room temperature prepared by conventional casting technique are shown in Figure 11. The cycles were run galvanostatically with the same current density during charge and discharge. As seen in this figure, good cell capacity can be achieved at a low discharge rate (5 $\mu A/cm^2$). However, at higher rates the capacity drops significantly, presumably due to the high resistance of the electrolyte/electrode interfaces. Two plateaus characteristic for the $Li/Li_xMn_2O_4$ system are present at low current density. At higher current densities, however, the high-voltage plateau is absent, indicating incomplete cathode utilization.

In Figure 12, the effect of current density on cell capacity for the cells prepared by ultrasonic spray is shown to be similar to that for cells prepared by casting. Figure 13 shows this similarity at low current density (5 $\mu A/cm^2$). At a higher current density (10 $\mu A/cm^2$) cells prepared by ultrasonic spray perform slightly better than cells prepared by casting. Specifically, cell capacity is slightly higher and some of the upper plateaus remain in the discharge curve of ultrasonically sprayed cell. This test shows, that while the charge-discharge characteristics of the cell mainly determined by interfacial resistance, reduction in the electrolyte layer thickness leads to some improvement in cell performance.

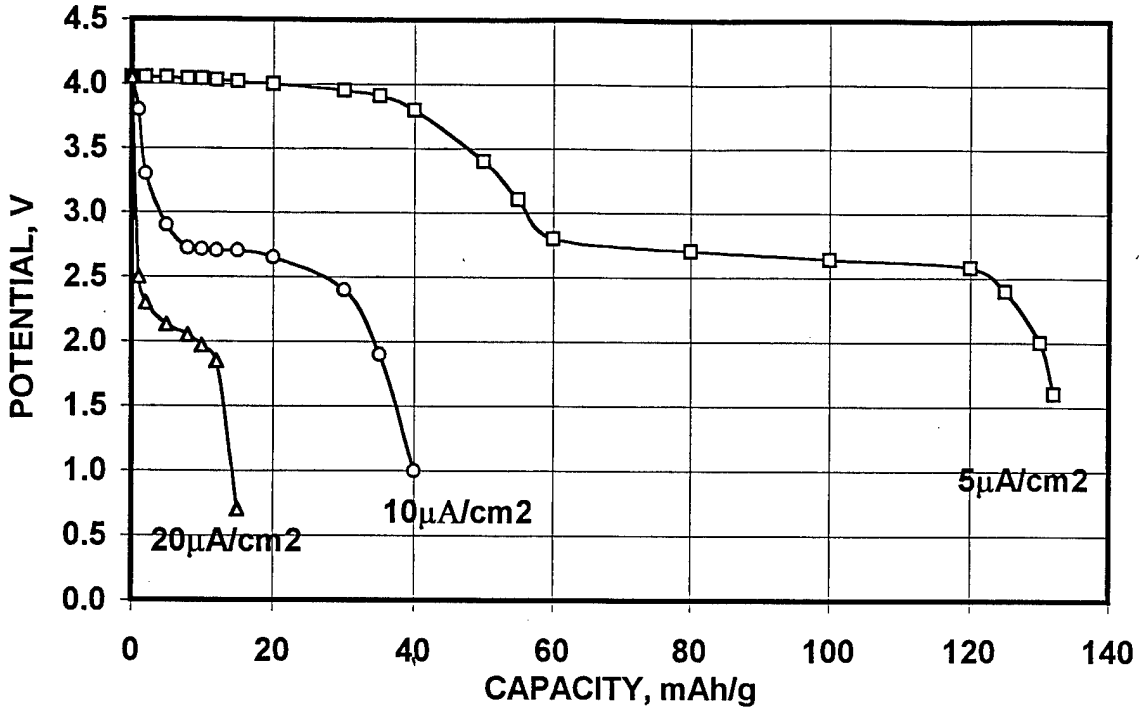

Figure 11. Effect of Current Density on Li/(a-PEO)$_{38}$Li[Al(OSiEt$_3$)$_4$]/ LixMn$_2$O$_4$ Cell Capacity. Electrolyte and cathode were prepared by casting.

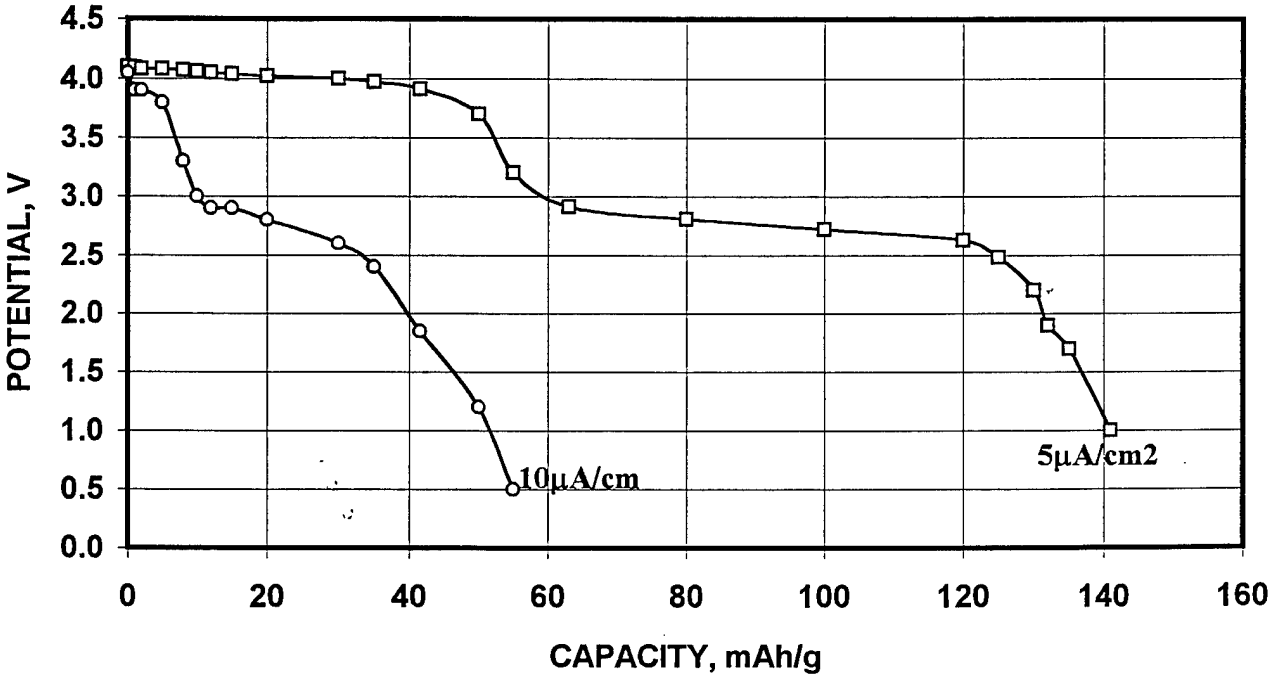

Figure 12. Effect of Current Density on Li/(a-PEO)$_{38}$Li[Al(OSiEt$_3$)$_4$]/ LixMn$_2$O$_4$ Cell Capacity. Electrolyte and cathode were prepared by ultrasonic spray.

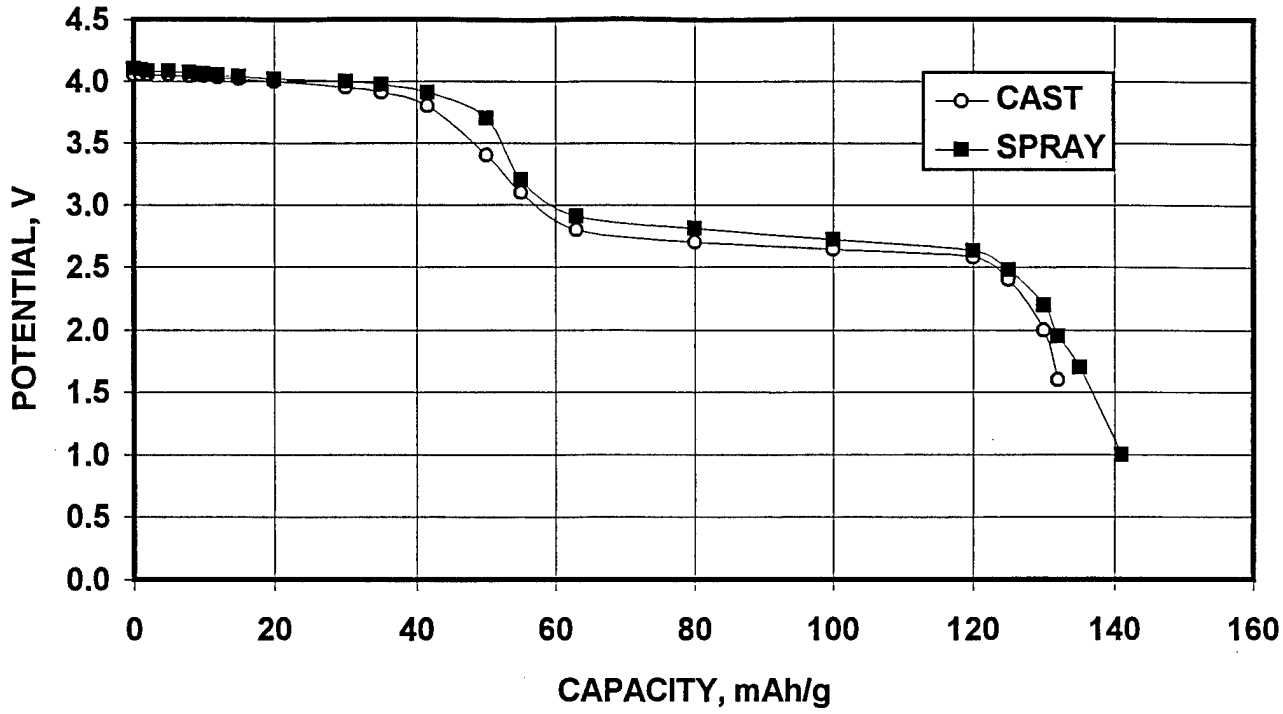

Figure 13. Discharge of Li/(a-PEO)$_{38}$Li[Al(OSiEt$_3$)$_4$]/ LixMn$_2$O$_4$ cells. Current density 5 μA/cm^2.

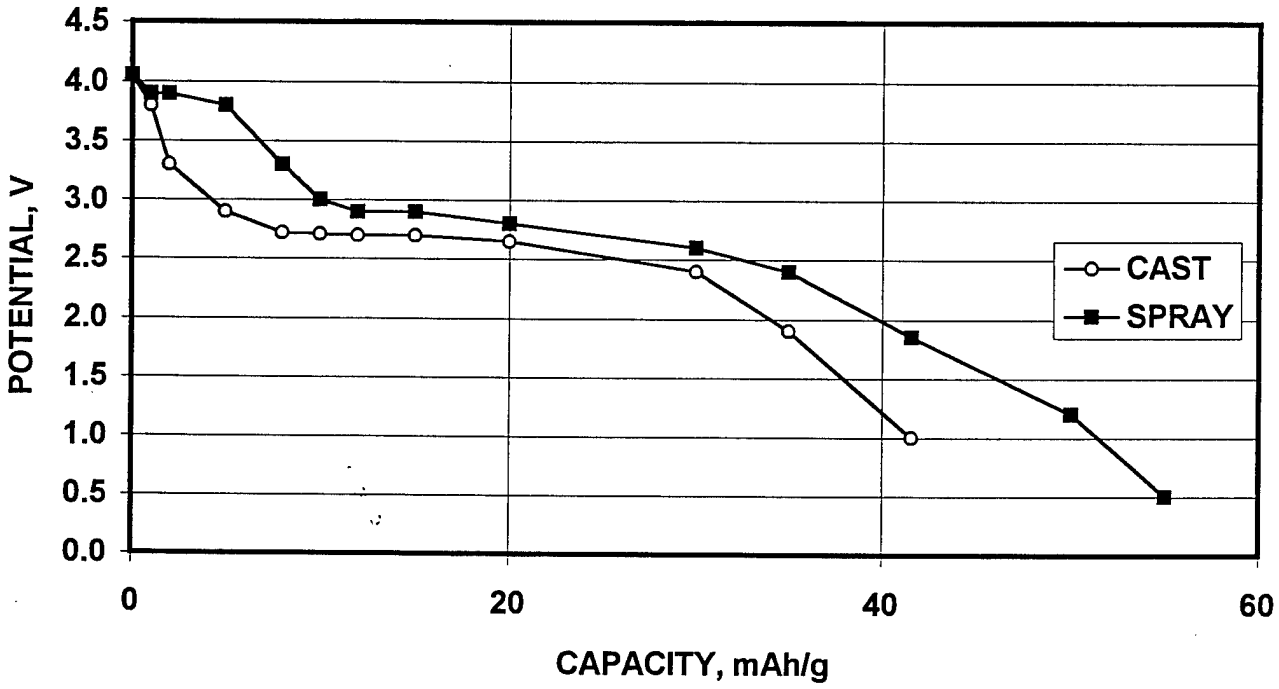

Figure 14. Discharge of Li/(a-PEO)$_{38}$Li[Al(OSiEt$_3$)$_4$]/ LixMn$_2$O$_4$ cells. Current density 10 μA/cm^2.

Figure 15 presents the results of repeated cycling of cell prepared by casting technique at 5 $\mu A/cm^2$ and at room temperature. The discharge curves indicate the full rechargeability of the cell to 4 V, but show sharp losses in capacity during extended cycling. This degradation of cell performance is attributed to passivation of the lithium electrode which was observed to be colored upon inspection of disassembled cells.

Similar degradation of the cell prepared by ultrasonic spray is evident in Figure 16. When data for two cells are compared (Figure 17), it is obvious that while there is degradation in the performance of both cells during extended cycling, the cell prepared by ultrasonic spray degraded slightly less than cell prepared by conventional casting technique.

Galvanostatic cycling of the cells prepared with this electrolyte by casting and ultrasonic spray gave erratic but promising performance. In future work, the variables that affect this performance should be studied in more detail. Also the nature of the apparent resistive interfacial layer needs to be identified by a range of element and molecule-specific spectroscopies including surface IR and Raman spectroscopy.

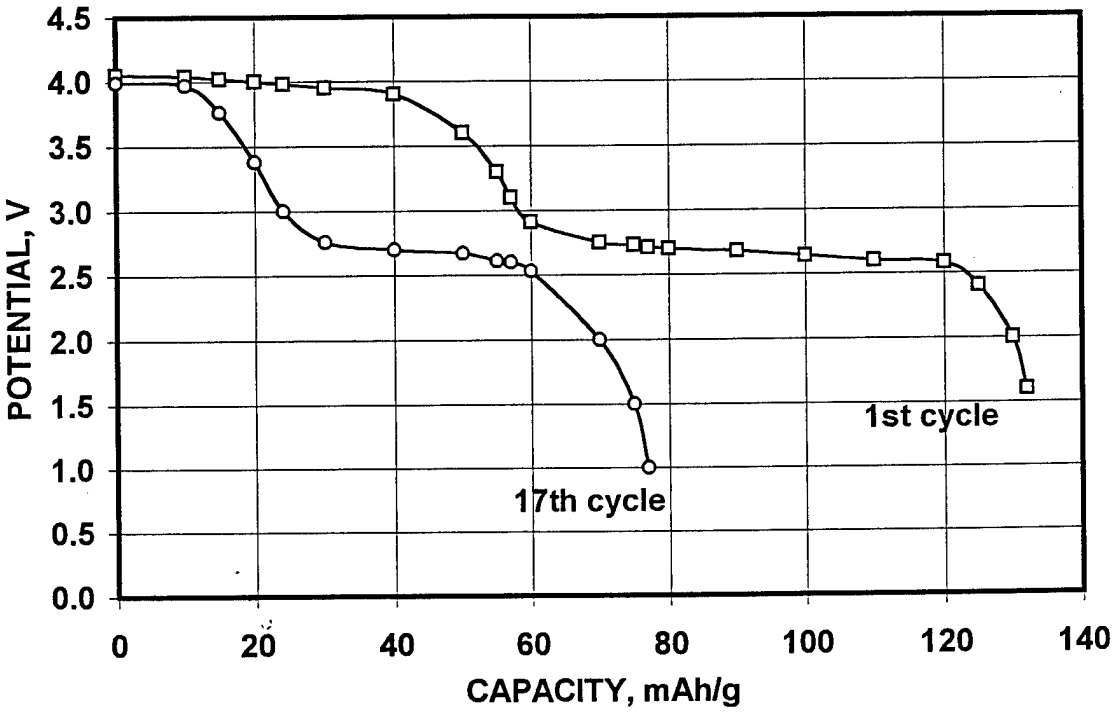

Figure 15. $Li/(a\text{-}PEO)_{38}Li[Al(OSiEt_3)_4]/ LixMn_2O_4$ cell capacity after repeated cycling at 5 $\mu A/cm^2$. Electrolyte and cathode were prepared by casting.

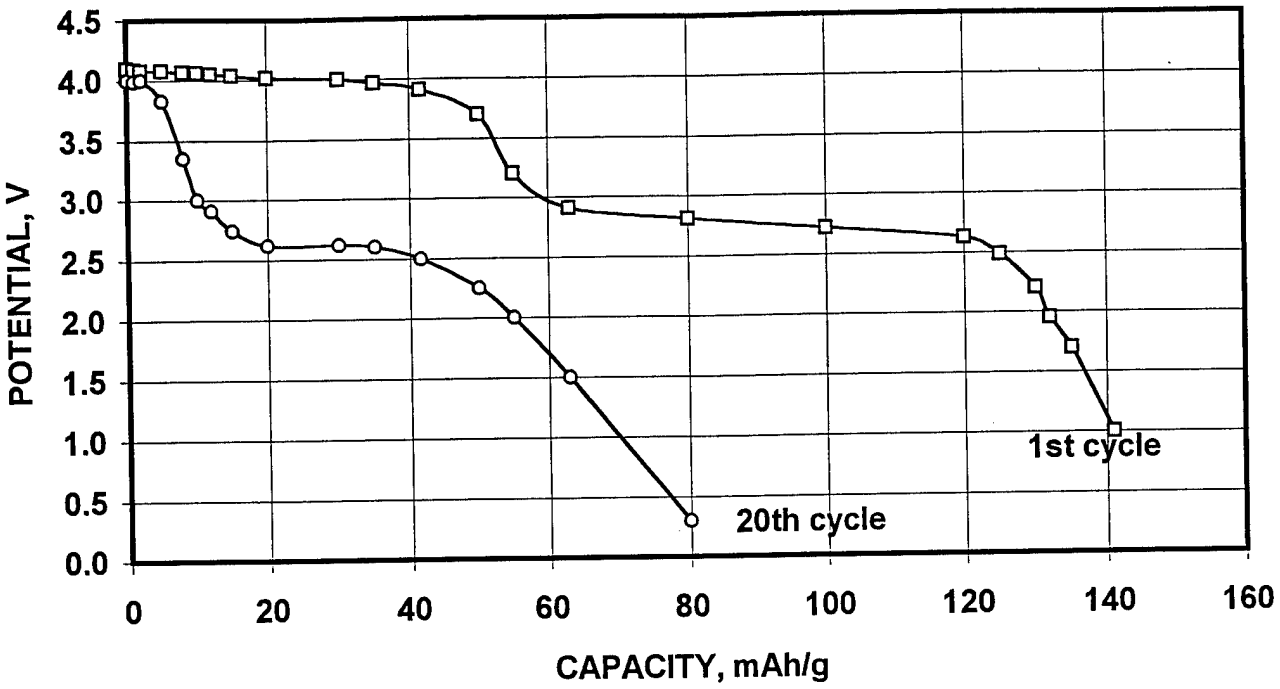

Figure 16. Li/(a-PEO)$_{38}$Li[Al(OSiEt$_3$)$_4$]/ LixMn$_2$O$_4$ cell capacity after repeated cycling at 5 μA/cm^2. Electrolyte and cathode were prepared by ultrasonic spray.

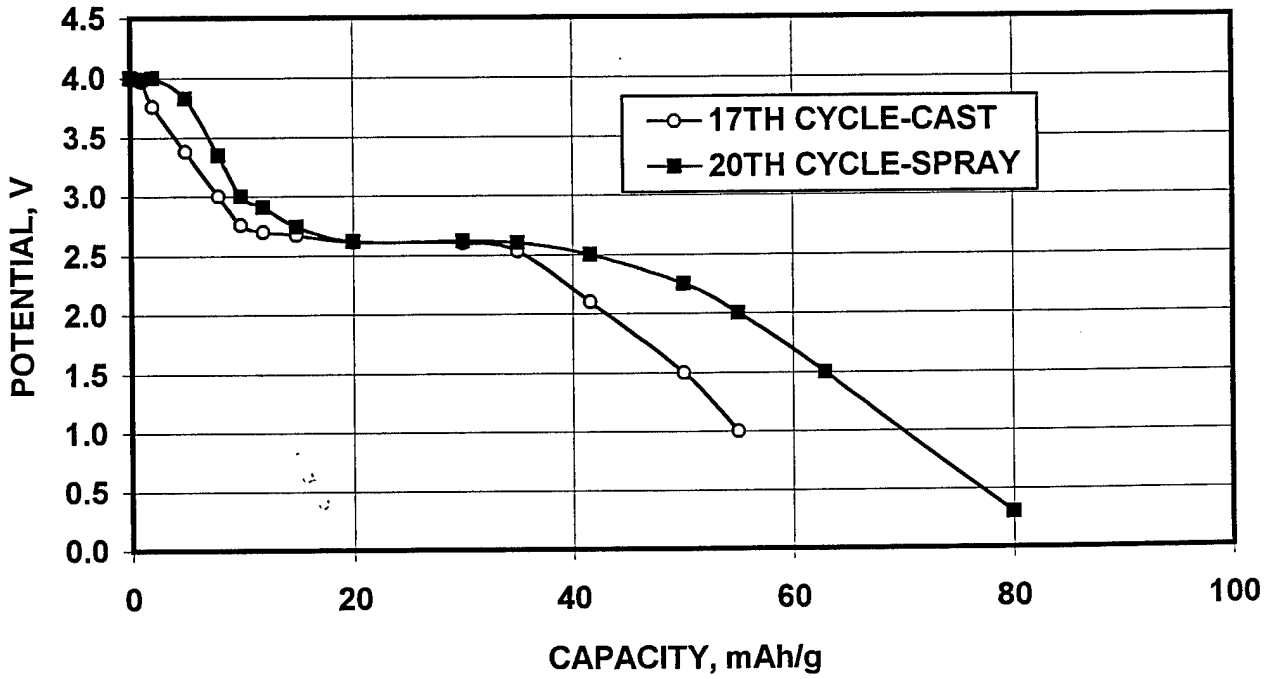

Figure 17. Discharge of Li/(a-PEO)$_{38}$Li[Al(OSiEt$_3$)$_4$]/ LixMn$_2$O$_4$ cells. Current density 5 μA/cm^2.

4.2. Li/(MEEP)$_4$LiCF$_3$SO$_3$/Li$_x$MnO$_2$ Cells

The 3 V cathode material, Li$_x$MnO$_2$, was used in cells with (MEEP)$_4$LiCF$_3$SO$_3$ because a cyclic voltammogram (Figure 18) indicated low stability of this electrolyte at higher potentials. Figure 19 shows that cells prepared by casting and containing MEEP-salt complex perform much better than cells containing the a-PEO-aluminosilicate complex. Higher current densities can be used during discharge of these cells. However, the increase in discharge rate lowers cell capacity (118 mAh/g at 20 μA/cm^2 and 73 mAh/g at 30 μA/cm^2). The reduction of the cell capacity with increased current density is probably the result of incomplete cathode utilization.

Figure 20 demonstrates that cells that contain (MEEP)$_4$LiCF$_3$SO$_3$ electrolyte and prepared either by casting or by ultrasonic spray perform practically the same at discharge current density of 20 μA/cm^2.

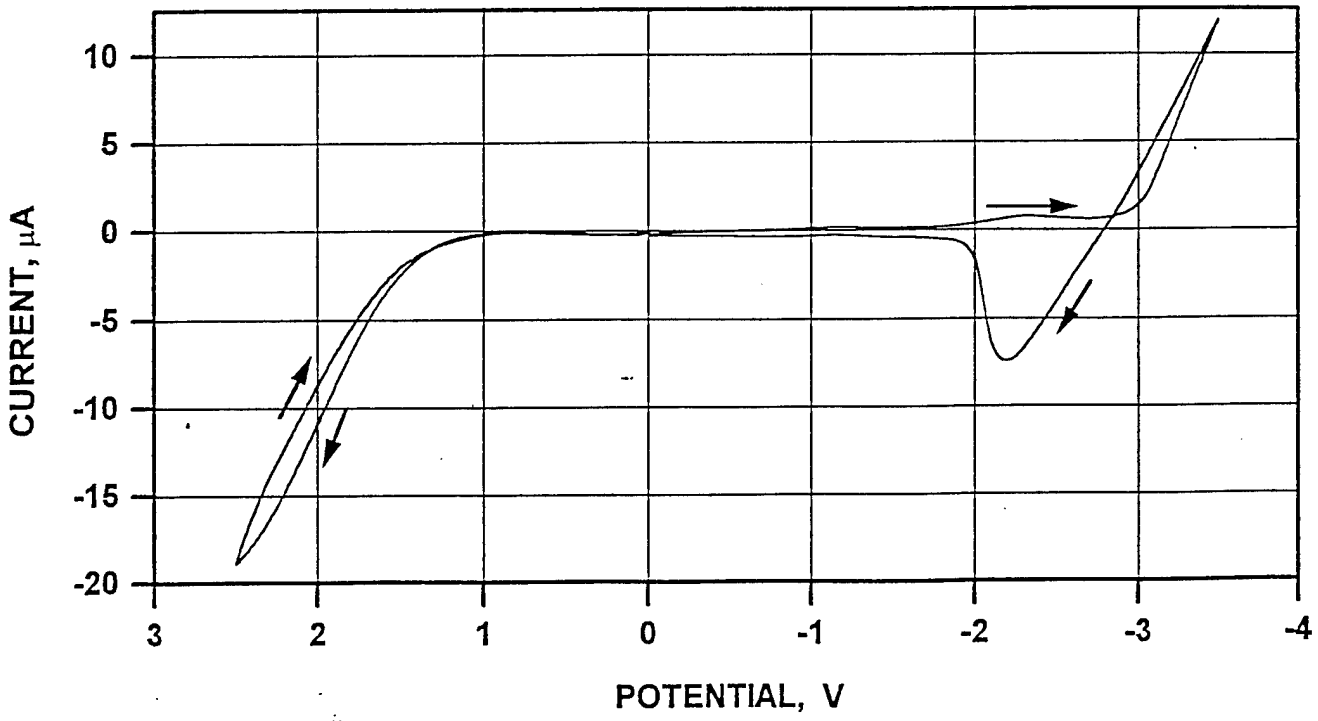

Figure 18. Cyclic voltammogram of Li/(MEEP)$_4$LiCF$_3$SO$_3$. Scan rate 20 mV/sec.

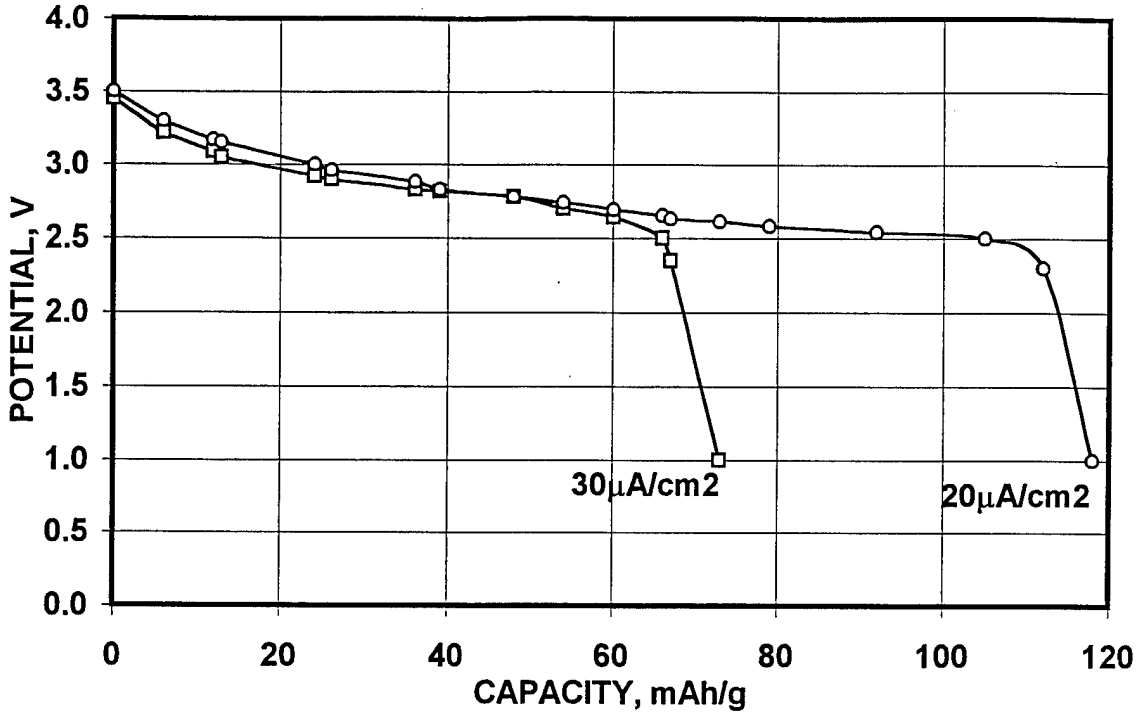

Figure 19. Discharge of $Li/(MEEP)_4LiCF_3SO_3/Li_xMnO_2$ cell. Cell prepared by casting.

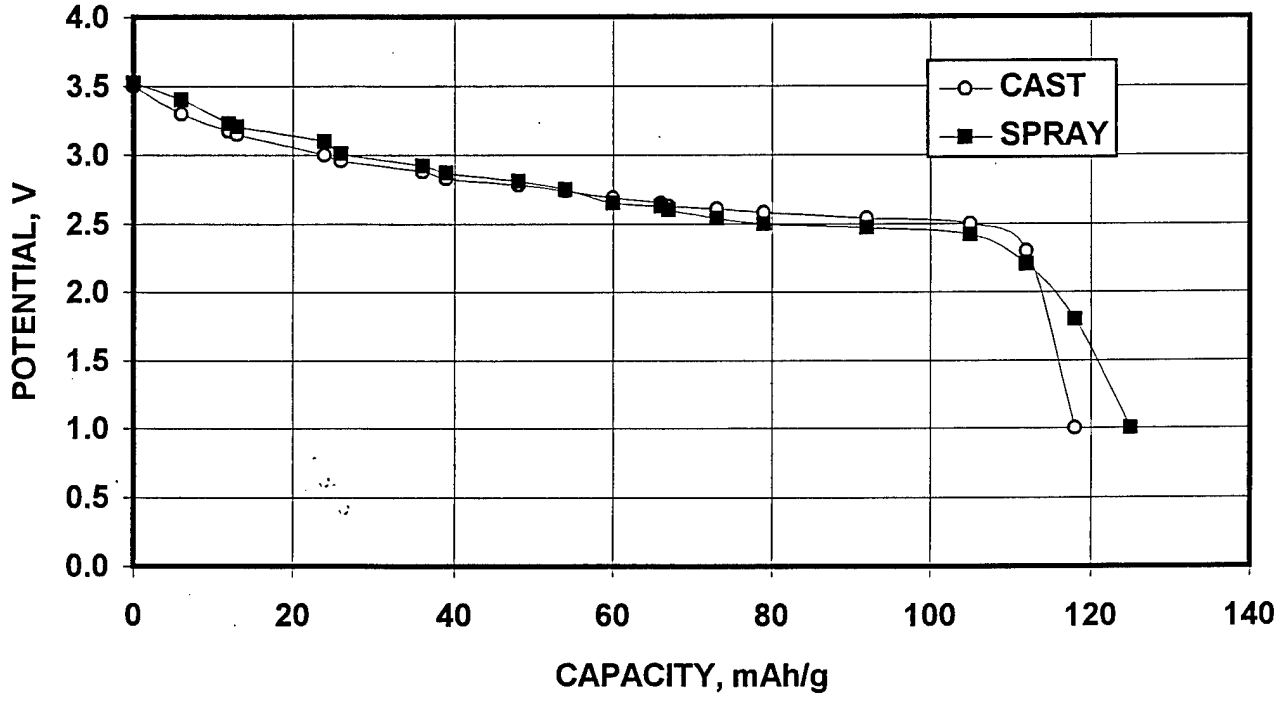

Figure 20. Discharge of $Li/(MEEP)_4LiCF_3SO_3/Li_xMnO_2$ cells. Current density 20 $\mu A/cm^2$.

A drop in capacity for cells prepared by casting was observed during repeated charging and discharging as shown in Figure 21. In the first cycle, the capacity of this cell was 122 mAh/g, and after the third cycle the cell capacity was reduced to 105 mAh/g. Also, the MEEP-salt complex did not form a rigid film, and creep of the electrolyte film was detected. As a rule, this deformation lead to a short circuit after a few charge/discharge cycles. The cells that were prepared by ultrasonic spray also failed due to creep of the electrolyte film.

AC impedance tests performed on symetrical cells with Li electrodes (Figures 22, 23) indicate that the total cell resistance increases with time. The Li-electrolyte interface resistance steadily increases with time while the bulk resistance slightly decreases. The increase in interface resistance indicates the formation of passive products on the Li surface. Reduction of the bulk resistance of the MEEP-salt electrolyte is probably due to creep of electrolyte film leading to thinner electrolyte films.

It is obvious that the MEEP-salt complex has good potential for application in lithium-polymer-electrolyte batteries. However, this potential may be realized only after problems of the low dimentional stability of MEEP and reactivity of MEEP or impurities in MEEP with Li are resolved. Appropriate spacer materials or cross-linked MEEP should overcome the problem of dimensional stability.

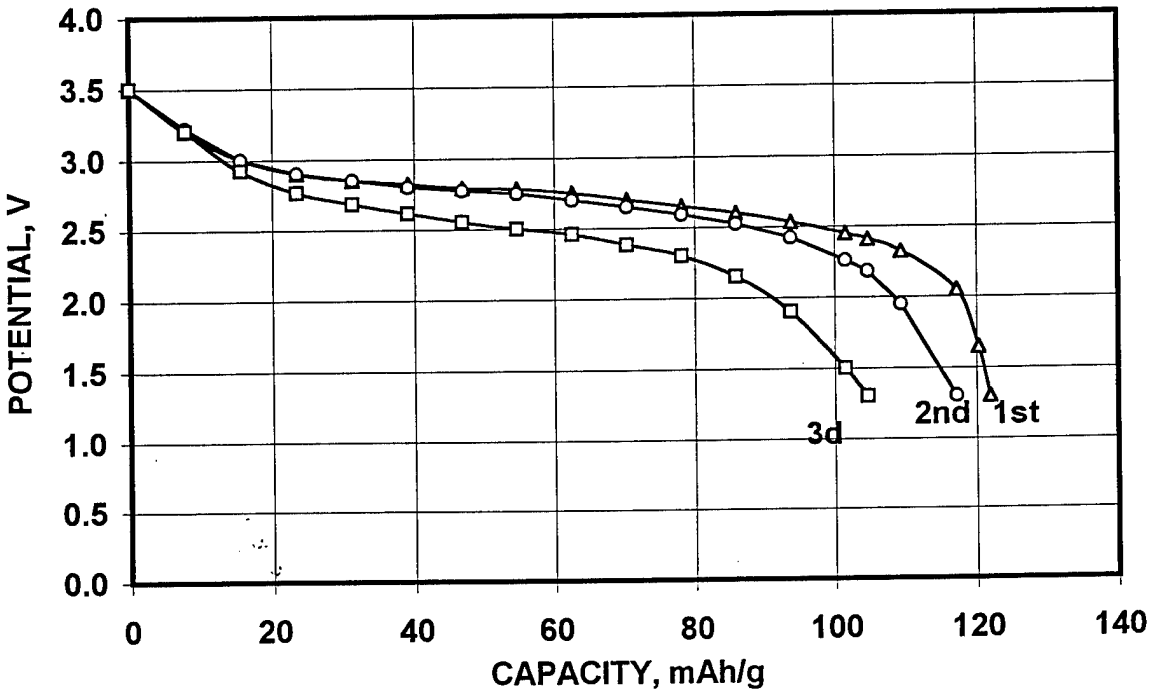

Figure 21. $Li/(MEEP)_4LiCF_3SO_3/Li_xMnO_2$ cell capacity after repeated cycling at 20 $\mu A/cm^2$. Cell prepared by casting.

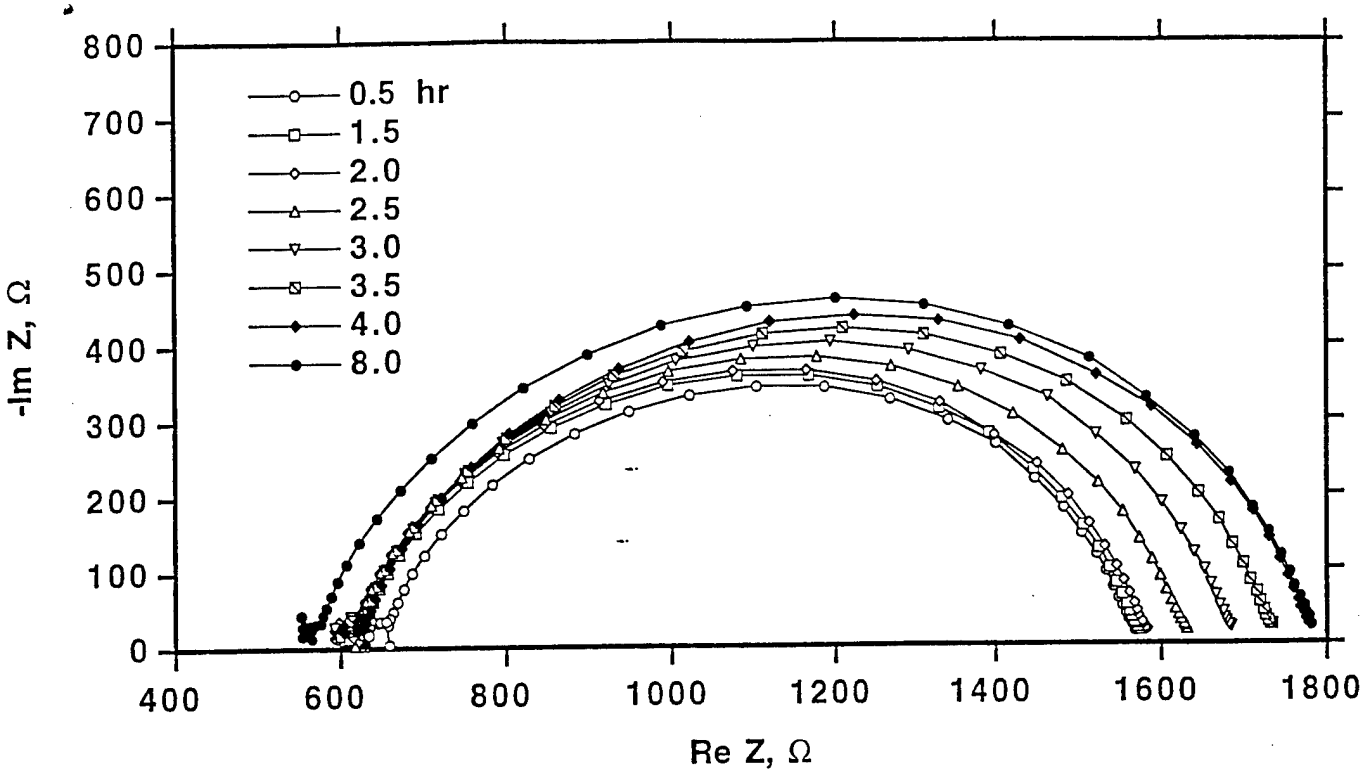

Figure 22. AC impedance spectra for a symmetrical Li/$(MEEP)_4LiCF_3SO_3$/Li Cell.

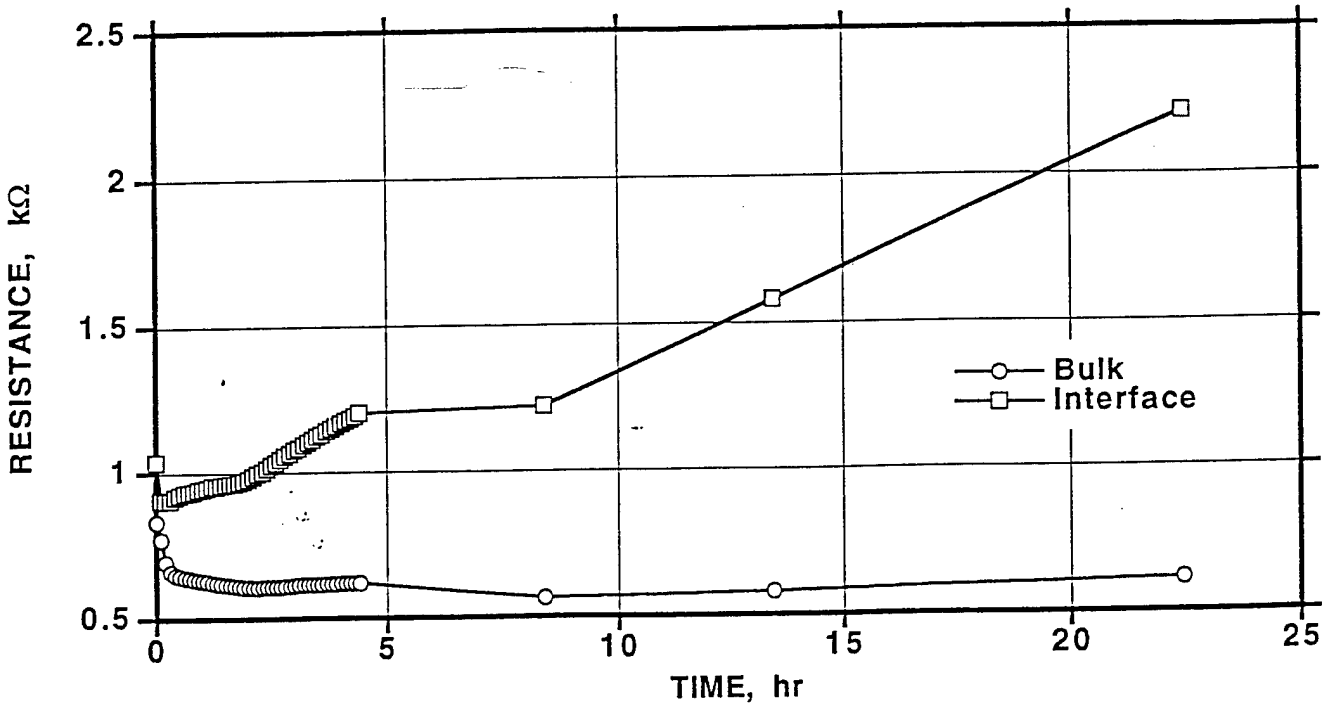

Figure 23. Change in the Li/$(MEEP)_4LiCF_3SO_3$/Li cell resistance.

4.3. Aluminosilicate Polyelectrolyte

As previously mentioned, the lack of solubility for cross-linked aluminosilicate polyelectrolyte, required film formation by pressing the polymer at 80°C. The films thicknesses were in the 100-120mm. Thinner films can be produced by casting or ultrasonically spraying linear aluminosilicate polyelectrolyte that may be synthesized in the manner similar to the synthesis of crosslinked polyelectrolyte studied in this project.

The charge/discharge characteristics of cells containing the aluminosilicate polyelectrolyte could not be determined at room temperature due to the lack of good quality films with thickness less than 100 mm. The thinner films should be produced by spraying similar polyelectrolyte linear polymers which should dissolve in organic solvents.

The conductivity of the aluminosilicate polyelectrolyte with cryptand, [2.2.2] (4,7,13,16,21,24-hexaoxa-1,10-diazabicyclo [8.8.8]hexacosane), and without cryptand was measured (Figure 21). It is evident that this polyelectrolyte has low conductivity at room temperature, but the conductivity improves by more than one order of magnitude when the cryptand is added. This is attributed to the decrease in ion pairing between the bound anion and encapsulated by the cryptand mobile cation. The general indication from these studies is that the aluminosilicate forms much stronger ion pairs than we had expected, although cryptands and plasticizers may produce acceptable performance.

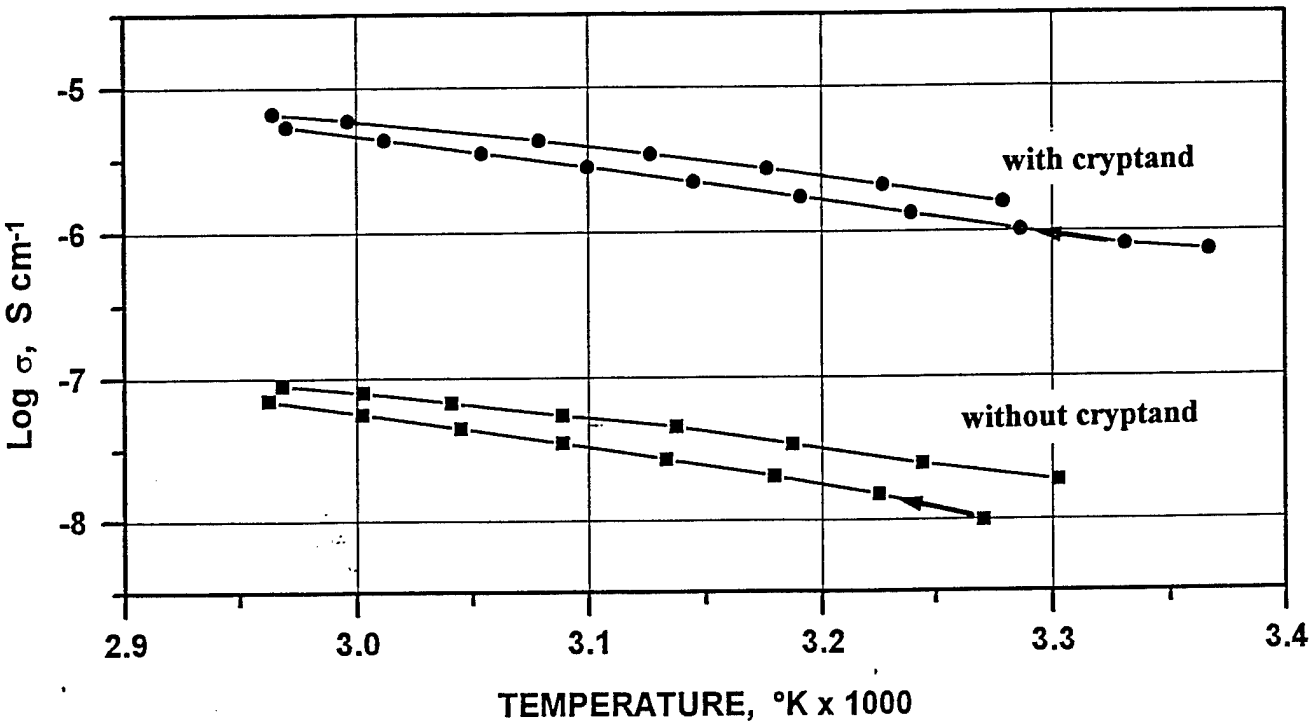

Figure 24. Conductivity of aluminosilicate polyelectrolyte with [2.2.2] (4,7,13,16,21,24-hexaoxa-1,10-diazabicyclo [8.8.8]hexacosane) cryptand and without cryptand.

SUMMARY

New polymer electrolytes (polymer-salt complexes) and aluminosilicate polyelectrolyte were synthesized, analyzed and tested in Li cells. Cells were prepared by casting and ultrasonic spray. Ultrasonic spray did not lead to the fragmentation of the polymer. Optimal concentrations of polymer in solvents for electrolyte and cathode film morphology was determined. Performance of cells prepared by ultrasonic spray was slightly better than that of cells prepared by casting. The primary limitations to cell performance were high cell resistance, apparent interfacial reactions between polymer-electrolyte and lithium, and dimensional instability (creep) of MEEP. Improvement in cell performance can be achieved by the use of spacers or crosslinking the MEEP to improve the dimensional stability of the electrolyte and by the addition of cryptands and plasticizers to increase ambient-temperature conductivity of polyelectrolytes.

REFERENCES

1. A. Hooper, in Solid State Batteries, C.A.C. Sequeira and A. Hooper, eds., Martinus Nijhoff Publishers, 1985, 399.
2. M.B. Armand, ibid., 363.
3. J. R. MacCallum and C. A. Vincent, in Polymer Electrolyte Reviews, Elsevier, Barking, 1987, 1989, Vol. 1 and 2.
4. S. Ganapathiappan, K. Chen, D.F. Shriver, Macromolecules, 1988, 21, 2299.
5. K. E. Doan, M. A. Ratner, D. F. Shriver, Chem. Mater. 1991, **3**, 418.
6. K. Chen, S. Ganapathiappan, D. F. Shriver, Chem. Mater., 1989, *1*, 483.
7. K. Chen, K. E., Doan, S. Ganapathiappan, M. A. Ratner, D. F. Shriver, in Proc. Mater. Res. Soc. Symp., Solid State Ionics II, Vol. 210, Nazri, G., Huggins, R.A., Balkanski, M., Shriver, D.F., eds., 1991, 215.
8. K. E. Doan, B. J. Heyen, M. A. Ratner, D. F. Shriver, Chem. Mater., 1990, *2*, 539.
9. G.C. Rawsky, K.J. Henretta, R. Lowrey, D.F. Shriver, S. Vaynman, in Proc. Mater. Res. Soc. Symp., Materials for Electrochemical Energy Storage and Conversion - Batteries, Capacitors and Fuel Cells", Vol. 393, D.H. Doughty, B. Vyas, J.R. Huff, eds., 1995, pp. 189.